Applied Thermal Engineering 111 (2017) 369–376

Contents lists available at ScienceDirect

Applied Thermal Engineering

journal homepage: www.elsevier.com/locate/apthermeng

Research Paper

Methodology to construct full boiling curves for refrigerant spray cooling

Sivanand Somasundaram [1], A.A.O. Tay *

Department of Mechanical Engineering, National University of Singapore, Singapore

HIGHLIGHTS

- Transient temperature measurements for a liquid nitrogen spray beyond CHF were made.
- Inverse heat transfer techniques applied to obtain instantaneous heat flux and temperature.
- Methodology to construct the boiling curve beyond CHF is discussed.

ARTICLE INFO

Article history:
Received 18 March 2016
Revised 19 September 2016
Accepted 20 September 2016
Available online 21 September 2016

Keywords:
Inverse heat conduction
Boiling curve
Liquid nitrogen

ABSTRACT

This paper proposes application of sequential function specification method to solve the inverse heat conduction problem to obtain instantaneous surface heat flux from transient temperature measurements. Transient temperature measurements beyond critical heat flux are obtained for a copper block being cooled by a liquid nitrogen spray. A method to construct the boiling curve beyond CHF is discussed. This method help in estimating the heat flux at various superheats even in the transition and film boiling region which is otherwise difficult to estimate.

1. Introduction

Film boiling is encountered in various applications like metallurgy, refrigeration, chemical and power engineering, etc. In particular knowledge of film boiling properties of coolants is of importance for nuclear reactors to assess the safety of nuclear reactor designs. Generally experimental boiling curves are obtained only until critical heat flux (CHF) as beyond this heat flux there is a vapor blanket on the surface and there is a thermal runaway situation. So conventional method of experimentation fails in the regime beyond CHF. Conventional experimental set up [1] involves controlled heat flux where heat flux is slowly increased and a stable steady state is obtained for each heat flux. But in such a set up beyond CHF, there is indefinite temperature rise. Another alternative is to have temperature controlled system [2], which would need a pressurized two phase liquid boiler to produce different temperatures. Such a system is complicated and expensive. Previous studies or reports in literature [3–10] concern mainly with extraction of boiling curves for pool boiling. Full boiling curve of saturated methanol was reported [3] for horizontal cylinders under pool boiling conditions. The possibility of cooling a superconducting magnet using liquid nitrogen, led to a report [4] of forced convection heat transfer study of liquid nitrogen inside horizontal tubes. But the study was limited to near nuclear boiling regime. Transient study of pool boiling of liquid hydrogen from a flat surface was reported [5] but limited until the critical heat flux. Numerical simulation and experiments of boiling of various cryogenic liquids were studied [6] to understand the pool boiling mechanism. Transition boiling and film boiling of FC-72 from horizontal cylinders and wires under pool boiling conditions were reported in [7]. Effect of heater orientation in liquid nitrogen pool boiling was reported in [8]. The optimal geometry of tube bundle for nucleate boiling of liquid nitrogen (over a tube bundle) was studied and reported in [9]. All regimes – nucleate boiling, transition and film boiling were reported in [10] for liquid nitrogen pool boiling over a thin wire. In summary there has been numerous studies of different cryogenic fluids under pool boiling conditions. The very limited reports on forced convection of cryogenic liquids do not fully cover the full boiling regime due to the experimental complexity at film boiling conditions. And in particular there are

* Corresponding author at: EA-07-19, Mechanical Engineering Department, Engineering Drive 1, National University of Singapore, Singapore 119260, Singapore.

E-mail addresses: sivanand@smart.mit.edu (S. Somasundaram), mpetayao@nus.edu.sg (A.A.O. Tay).

[1] Presently at Singapore-MIT Alliance for Research and Technology Centre (SMART), Low Energy Electronic Systems (LEES), 1 CREATE Way, #05-09/10/11 Innovation Wing, Singapore 138602, Singapore.

http://dx.doi.org/10.1016/j.applthermaleng.2016.09.112
1359-4311/

Nomenclature

d	diameter (mm)	S	error function
h	heat transfer coefficient (W/m^2 K)	T	temperature (°C)
H	height of nozzle from chip/copper block (mm)	t	time (s)
h_{fg}	latent heat of vaporization (J/kg)	T_{ij}	temperature of jth node at ith time step
k	thermal conductivity (W/m K)	T_m	temperature in time interval $\lambda_{(m-1)} - \lambda_m$
L	length of equivalent copper block (mm/m)	x	distance along copper block from top surface (mm/m)
N	number of spatial nodes in copper block	y	measured temperature
q	heat flux (W/m^2)	ϕ	sensitivity coefficient
Q	heat (W)	α	thermal diffusivity (m^2/s)
q_m	heat flux in time interval $\lambda_{(m-1)} - \lambda_m$	$[\lambda_{(m-1)} - \lambda_m]$	time interval at time t_m
r	number of future time steps	ρ	density (kg/m^3)

no reports for generating full spray boiling curves for cryogenic fluids.

So this present work proposes that measurement of transient temperature readings of a thermal run away beyond CHF, and transient temperature readings while cooling down from a high temperature to the nucleate boiling region is sufficient to estimate the boiling curve beyond CHF. There is a report [11] of similar approach to extract the boiling curve of water, but involves a complicated experimental set up, as there is a need to create a symmetrically cooled target by having twin sprays - force convection boiling on two sides of the target, in order to simplify mathematical treatment. Also the previous method required high frequency (1000 Hz) data acquisition without much noise. The present work demonstrates a novel and easyway to implement the method. The requirements of the experimental set up are simple and easy but the demonstration in the present work is done using liquid nitrogen, as this was part of a bigger research study which involved liquid nitrogen sprays. So there were some additional experimental set up required to get saturated liquid nitrogen, but for other fluids this additional experimental setup might not be required.

2. Experimental set up

A custom experimental rig was built to study liquid nitrogen spray boiling. The transient data obtained from this rig was processed to obtain the full boiling curve.

The schematic diagram of the experimental set up, showing important sensors and equipment, is shown in Fig. 1. The commercially available high pressure LGC (liquid gas cylinder), which stored liquid nitrogen at 230 psi was rented from the local supplier SOXAL. The internal cylinder pressure is used for pumping the liquid. It is to be noted that since the pressure of the liquid gas mixture is higher in the LGC tank compared to atmospheric pressure, the liquid is at the saturation temperature corresponding to the cylinder pressure and is typically at about −160 to −165 °C. When the high pressure, high temperature (1.58 MPa, −165 °C) liquid is throttled to a atmospheric pressure in the nozzle, the gaseous component is high. To overcome this problem, the liquid withdrawn from the cylinder is cooled in a heat exchanger. Since the cylinder pressure varies depending on the heat leak to the cylinder and the withdrawal rate, a pressure regulator (REGO) was fixed at the outlet of the cylinder and set at 125 psi. This high pressure, high temperature (relative to 77 K) liquid was sub-cooled in a custom-built heat exchanger. The heat exchanger was a coiled tube immersed inside liquid nitrogen filled Dewar (an insulated container to hold refrigerants). The Dewar was constantly topped up with liquid nitrogen from a commercially available 22 psi LGC tank (not shown in Fig. 1). The liquid exiting from the heat exchanger is at high pressure and at about 77–78 K. The sub-cooled liquid is transferred into the spray chamber and the distance between the heat exchanger and the spray chamber was reduced as much as possible and was approximately 300 mm, to reduce heat gain from environment 25 mm thick polyurethane insulation. All transfer lines are insulated using to reduce heat leak into the lines. A solenoid valve is placed before the entry into the spray chamber. The solenoid valve (D2062 series, Gems sensors) was compatible to liquid nitrogen temperatures because of the PTFE lining. It had an orifice diameter of 3.175 mm and a response time of 40 ms and was used to switch on/off the spray.

The spray chamber is a custom-built, double-layer vacuum-jacketed stainless steel cylindrical chamber. The vacuum jacket helps to prevent condensation on the view ports. The nozzle used was TG SS 0.7 (Spraying Systems Company) which is a full cone nozzle having an orifice diameter of 0.76 mm. A 25 × 25 mm^2 copper block served as a simulated IC chip. The heater block accommodated four 250 W cartridge heaters. It was insulated by a Teflon block on all the four sides and at the bottom. The Teflon block near the top surface had sloping edges at 45° angle to promote better drainage of the coolant. The temperatures were measured in the copper block using T type thermocouple sheathed probes (AWG 30 wire in 1.6 mm stainless steel sheath) with exposed junction for faster response to transient changes in temperature. The response time is estimated to be about 30 ms. There were three holes drilled in the Teflon housing and copper block to house the thermocouples. The thermocouples were inserted into their respective holes, which had tight fit tolerance. The measurement points of temperature were 2.8, 5.8, and 8.8 mm below the top surface at the central plane. The surface roughness of the copper surface was measured by a surface profilometer and the *Ra* value was about 0.5 μm. The chamber also had four screws to fix the position of the copper block precisely to align the copper block to the center of the nozzle/spray. The cartridge heaters were powered by a 1.5 kW DC power supply (AMREL SPS series 1.5 kW, 60 V, 25 A), which was connected to the computer through a GPIB cable to control the voltage supplied in the constant voltage mode.

The temperatures measured by the four thermocouples in the copper block, the nitrogen inlet pressure and temperature, chamber pressure and temperature were all acquired by a NI cDAQ system. A LabView program synchronized the measurements and stored all the values along with a time stamp. The program also calculated the surface temperature and actuated the valve to open or close.

The uncertainty in temperature measurement of the copper block temperature using thermocouples is estimated to be ±1 °C at liquid nitrogen temperatures. The uncertainty of thermocouple location in the copper block is 0.8 mm, half the diameter of the hole. The uncertainty in liquid temperature and ambient temperature, measured using RTD is about ±0.15 °C. The uncertainty in pressure measurement was about ±0.05 MPa, although accuracy

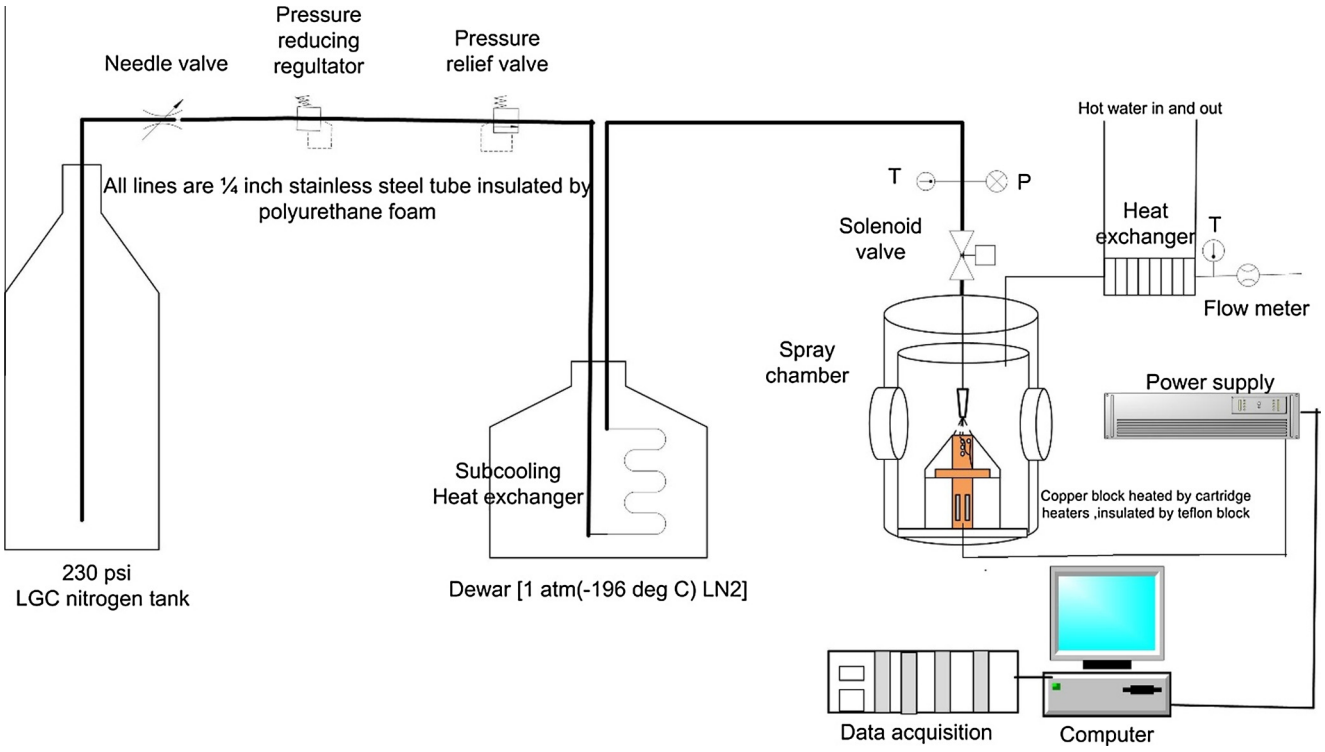

Fig. 1. Schematic of experimental setup to study liquid nitrogen sprays.

of pressure transducer is about ±0.01 MPa, because the transfer line was under fluctuations which are typical of a two phase flow. The nozzle to surface height has an uncertainty of ±0.5 mm.

The errors in voltage and current measurements were 0.2% of reading ±20 mV and 0.3% of reading ±20 mA, respectively. However the main uncertainty in the heat flux was from the heat loss calculations. The heat loss was estimated to be about 5% for experimental conditions where the surface temperature was low (77–100 K) with an estimated uncertainty of ±10% (by a detailed numerical simulation of the heater block). At very high elevated surface temperatures (100–293 K) the heat loss was very high (6–55% depending on the operating temperature) with an estimated uncertainty of ±10%. So the total uncertainty in estimation of heat flux removed is 2–3% for the lower range (77–100 K) and 3–6% for the higher range (100–293 K).

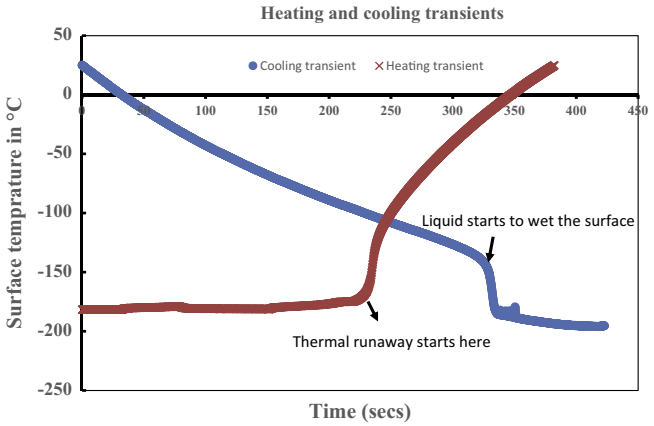

Fig. 2. Typical transient heating and cooling curves.

3. Experimental methodology

First the conventional steady state experiments were done using a constant flux mode and the steady state temperature was recorded. At one particular point when the CHF was reached, the temperature continued to rise rapidly, the heating rate was maintained until the surface temperature reached up to 20 °C. After which the power supply to the heaters were turned off, while the spray continued to be on until the surface temperature reached down to −196 °C. Both the heating transient and the cooling transient were recorded at time intervals of 100 ms. It took about 250 s for transient heating and about 500 s for transient cooling. It is observed that there is sudden change in temperature when the wall superheat is at about 50 K, which corresponds to the Leidenfrost point [12], at which the liquid starts/stops to wet the surface directly in cooling/heating. Fig. 2 shows typical transient heating and cooling curves. It is to be noted that during heating transient curve, the heater is on all the time with a heat flux corresponding to the minimum flux initiating CHF and during the cooling transient the heater is always off. The spray is ON at all times during both the transients.

To estimate the transient heat transfer coefficient as a function of the wall temperature, the inverse heat conduction problem was solved. The following sections define the inverse problem and the methodology taken to solve the problem.

4. Definition of the inverse problem

The thermal mass or specific heat of the copper block is large (approximately 109 J/K). So, a lumped heat capacity method is not applicable. To find the instantaneous heat transfer coefficient it is necessary to quantify the instantaneous heat flux through the top surface. In transient condition, the power supplied to the copper block partially exits out from the top surface and partially heats up the copper block.

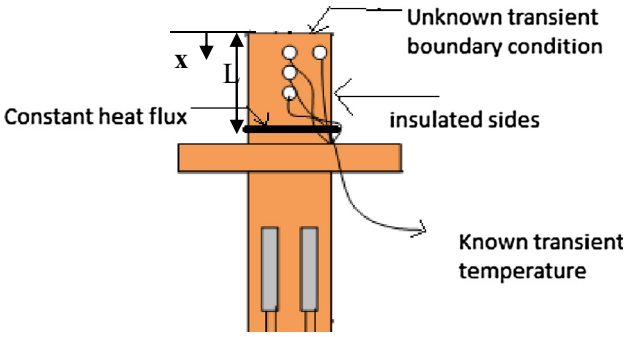

Fig. 3. Boundary conditions of the inverse problem.

The known boundary conditions and the unknown values are shown in the schematic in Fig. 3. Usually in a direct problem the boundary conditions are known and the solution of internal values is found. In the present problem as seen above, it is clear that the temperature transient (internal values) is known from experimental measurement and applied heat flux at the base is also known and the transient boundary value (heat flux and temperature) at the surface is to be found out. Similar methodology was applied to extract instantaneous heat transfer coefficients in intermittent sprays [13].

5. Model reduction

The inverse problem was solved by assuming the heat conduction to be one-dimensional as copper is a very good conductor and the sides have been well insulated.

A MATLAB code was written to solve a linear one-dimensional IHCP (Inverse Heat Conduction Problem) based on a sequential function specification method described below. The code used the finite difference method to discretize the one-dimensional heat equation.

$$\frac{1}{\alpha}\frac{\partial T}{\partial t} = \frac{\partial^2 T}{\partial x^2} + \frac{\dot{q}}{k} \tag{1}$$

$$\alpha = k/(\rho * C_p) \tag{2}$$

First order forward difference or Euler method was used for time discretization. The length of copper block considered for modeling was discretized into nodes numbered 1,2,…,j,…,N, with each node having size of Δx. It is assumed that the Nth node experiences a constant heat flux input of q_N and the 1st node experiences a transient heat removal described by q(t).The temperature at (i + 1)th time step is found using the temperature profile at ith step using the following discretized equations:

$$T_1^{i+1} = T_1^i + 2\Delta t\left[\frac{q(t)}{\rho c \Delta x} - \frac{\alpha}{\Delta x^2}\left(T_1^i - T_2^i\right)\right] \tag{3}$$

$$T_j^{i+1} = T_j^i + \frac{\alpha \Delta t}{\Delta x^2}\left[T_{j-1}^i - 2T_j^i + T_{j+1}^i\right] \tag{4}$$

$$T_N^{i+1} = T_N^i + 2\Delta t\left[-\frac{q_N}{\rho c \Delta x} + \frac{\alpha}{\Delta x^2}(T_{N-1}^i - T_N^i)\right] \tag{5}$$

Eqs. (3)–(5) are obtained by discretizing Eq. (1) and applying the appropriate boundary conditions at node 1 and N. Eq. (3) is for node 1, Eq. (4) is for interior nodes and Eq. (5) is for last node N. The heat flux entering or leaving the start and end nodes were treated as volumetric heat generation in these nodes. Even though the measurement time steps were about 100 ms, the time step Δt used to solve the transient heat equation was set to 1 ms in order to have a lower grid Fourier number. The heat flux estimation from the top surface was done at the instant when a set of readings were measured and it was assumed constant, until the instant when the next set of readings were measured.

6. Basis of sequential function specification method

The solution uses Duhamel's theorem as described by Beck [14]. However, a short summary of the same is described below followed by an explanation of how the methodology was applied to the present problem. Duhamel theorem utilizes a building block solution and the principle of superposition, assuming that the problem solved is linear, to obtain the temperature distribution spatially and temporally. The building block solution used is ϕ(x,t) which is the temperature rise at a point x at time t in a heat conducting body due to unit step heat flux as shown below

$$q(t) = 0 \text{ at } t \leqslant 0;\ q(t) = 1 \text{ at } t \geqslant 0 \tag{6}$$

The total time period is divided into equal intervals $0 - \lambda_1$, $\lambda_1 - \lambda_2, \ldots, \lambda_{(m-1)} - \lambda_m$ with each interval having a constant heat flux during that time interval. The corresponding heat flux during the interval $\lambda_{(m-1)} - \lambda_m$ is denoted by q_m, which may be regarded as the value of the heat flux at time $\lambda_{(m-1/2)}$. So if the body is initially at a uniform temperature of T_o and has a variable heat flux boundary condition, using Duhamel's theorem, it can be shown that

$$\begin{aligned} T(x,t_m) = T_0 &+ q_1[\phi(x,t_m - \lambda_0) - \phi(x,t_m - \lambda_1)] \\ &+ q_2[\phi(x,t_m - \lambda_1) - \phi(x,t_m - \lambda_2)] \\ &+ \cdots\cdots q_m[\phi(x,t_m - \lambda_{m-1}) - \phi(x,t_m - \lambda_m)]. \end{aligned} \tag{7}$$

The same equation can be written in short for temperature, T_m at time t_m and at a particular point x as

$$T_m = T_o + \sum_{n=1}^{m} q_n \Delta\phi_{m-n}$$

where (8)

$$\Delta\phi_i = \phi_{i+1} - \phi_i$$

$$\phi_i = \phi(x,t_i)$$

In sequential function specification, generally the heat flux components are known till time t_{m-1} and the estimation of heat flux components q at mth time step and future time steps are required. In a general case, there can be a known internal heat generation or there will be a known heat flux or known convection condition, at other boundaries say x = L. The final temperature at a given point at time λ_m will not only depend on $q_1, q_2, \ldots, q_m$ but also on known energy exchanges at other boundaries. Therefore, for general case it the above equation changes to

$$T_m = \hat{T}_{m|q_m=0} + \sum_{n=1}^{m} q_n \Delta\phi_{m-n} \tag{9}$$

where

$\hat{T}_{m|q_m=0}$ is the resulting temperature from all previous estimated heat flux components and with all other known energy exchanges. The future estimated heat flux components are set to zero.

For example

$\hat{T}_{m|q_m=0}$ is the temperature at time t_m due to all previous known heat fluxes $(q_1, q_2, \ldots, q_{m-1})$ and also due to known energy exchanges through other boundaries until time t_m. q_m is set as zero.

$\hat{T}_{m+1|q_m=q_{m+1}=0}$ is the temperature at time t_{m+1} due to all previous known heat fluxes $(q_1, q_2, \ldots, q_{m-1})$ and also due to known energy exchanges through other boundaries until time t_{m+1}. $q_m = q_{m+1} = 0$.

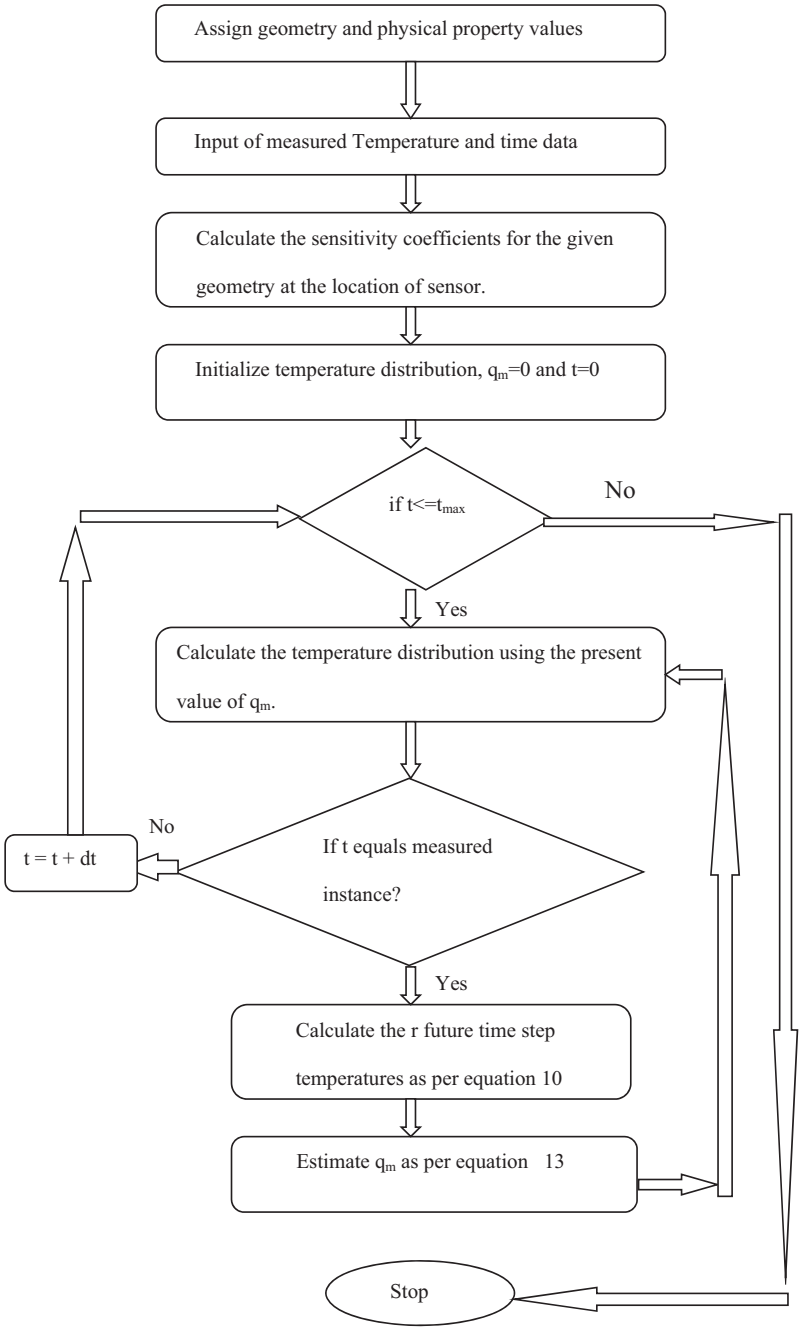

Fig. 4. Flowchart of sequential function specification method.

The q_m, q_{m+1}, etc. values are set to zero because the effect of q_m, q_{m+1}, etc. in the temperature is taken care in the second term of the Eq. (9).

Eq. (9) can be used to find the estimated future temperature in terms of q_m; If r is the number of future time steps, the sequential method of solving a function specification method involves the following steps.

a. The heat flux is known for time $t \leqslant t_{m-1}$ and a functional form for q(t) (which relates q_{m+1},q_{m+2}, etc. with q_m) is assumed for future time steps t_m, t_{m+1},. . .. . . ,t_{m+r-1}.
b. Based on the assumed heat flux values for future time steps, future temperatures are calculated using Eq. (9). The future temperatures are then a function of q_m, as other heat fluxes can be represented in terms of q_m using the assumed functional form, q(t). Then the square of the differences between the calculated future temperature and the measured temperature is set to a minimal value by finding an appropriate value of q_m.
c. Only q_m is retained.
d. The value of m is increased by one.
e. The same procedure is repeated for the next time step.

So in a constant heat flux functional form with r future time steps $q_m = q_{m+1} = \ldots = q_{m+r-1}$ and the general Eq. (9) for temperature at a future time step reduces to the following equation

$$T_{m+r-1} = \widehat{T}_{m+r-1|q_m=q_{m+1}=\ldots q_{m+r-1=0}} + (\phi_r * q_m). \quad (10)$$

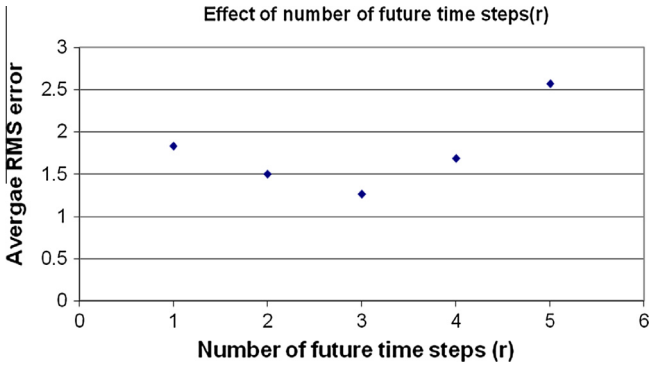

Fig. 5. Effect of number of future time steps.

Eq. (10) is obtained by using the relation

$$\phi_j = \sum_{i=0}^{j-1} \Delta\phi_i \tag{11}$$

The error function to be minimized is as follows

$$S = \sum_{i=1}^{r} \left(y_{m+i-1} - \widehat{T}_{m+i-1|q=0} - \phi_i * q_m \right)^2 \tag{12}$$

y_{m+i-1} is the measured temperature at the corresponding time.

Minimizing S with respect to q_m gives the following relation for q_m.

$$q_m = \frac{\sum_{i=1}^{r} \left(y_{m+i-1} - \widehat{T}_{m+i-1|q_m=0} \right) * \phi_i}{\sum_{i=1}^{r} \phi_i^2} \tag{13}$$

The flowchart of the algorithm, on which the MATLAB code is written, to solve the above described sequential function specification method is shown in Fig. 4. The effect of number of future time steps was observed, by calculating the mean square error between the actual temperature measured by the sensor and the temperature predicted by a forward heat conduction model. Temperature prediction was based on the estimated heat fluxes from the inverse heat conduction problem. The error as a function of number of future time steps is shown in Fig. 5 and it can be observed that the error reaches a minimum at point r = 3. Therefore, for this problem the suitable number of future time steps was chosen as three.

However the limitation is the need to know the exact thermal mass participating in the transient heating and cooling. Since there is a sudden and large increase in surface temperature, the transient heating or cooling of the copper block's thermal mass and insulation (Teflon) does play a role and quantifying its effect is critical in estimating the actual heat transfer through the top surface.

7. Results and discussion

The proposed solution to solve this problem is described in this section. The effect of actual heat loss/gain from the copper block to the adjoining heater structure, insulation and surroundings is to reduce/increase the surface temperature for a given heat flux and spray conditions. If a large copper block with no heat loss is modelled in the inverse problem being solved it will result in increase/decrease of transient surface temperature (compared to actual experimental conditions) during cooling/heating. Since the total measurement time is short (200–500 s), it is a valid assumption to model a slightly longer copper block, whose extra thermal mass will take into account the transient heat loss/gain. However if the assumed size is smaller compared to the actual equivalent size, then the heat transfer coefficients during transient heating will be higher than the actual value. This means that for an applied heat flux and measured temperature, the model would represent that less energy is used up for self-heating and large amount of heat is removed from the top boundary. Similarly during a cooling curve, during which heat supply is turned off, for a measured temperature drop, a smaller size of the equivalent copper block length would mean that the amount of heat flux removed is lower and would result in lower heat transfer coefficients.

So a smaller assumed length would result in higher heat transfer coefficients during transient heating and lower values during transient cooling. However the heat transfer coefficient is expected to be the same at a given surface temperature for the same flow conditions. So the length is varied until the heat transfer coefficients for heating and cooling converge. It should be noted that it is assumed that the heat transfer is more prominently one dimensional and the lateral conduction will not significantly affect the inverse heat conduction problem solved to estimate the transient heat flux removed at the top boundary.

L is the distance from the top surface to the bottom where a constant heat flux boundary condition is applied. Physically there is one real value for 'L'. However there is a virtual equivalent value of L which would be representative of the system for taking into account the thermal mass contribution from surrounding insulation. So "actual/ representative" 'L' is the length of copper block which will have equivalent thermal mass to account for heat gain/loss by the neighbouring insulation.

Based on the assumption that the walls of copper block are perfectly insulated and the heat conduction is 1D, for a given length L of the block (which will determine the thermal mass participating and hence the instantaneous heat flux being removed) the inverse heat conduction problem was solved using a Matlab code. The method used to solve the problem is Beck's [14] sequential function specification method. A constant heat flux function form was assumed between two measurements and three future time steps were used in solving the problem.

For analysis, experimentally measured data, the above mentioned nozzle with orifice diameter of 0.76 mm was used with an inlet pressure of 0.65 MPa, with nozzle to heater height of 36 mm. the flow rate was 26 kg/h. Both the heating and cooling curves (heat flux vs. ΔT) were found and this was repeated for increasing values of L and at a particular value of L both the curves were close to each other as shown in Figs. 6 and 7. It can be seen that for L = 0.08 m, at a given wall temperature the heat flux values are higher for heating compared to cooling. It is also seen that for

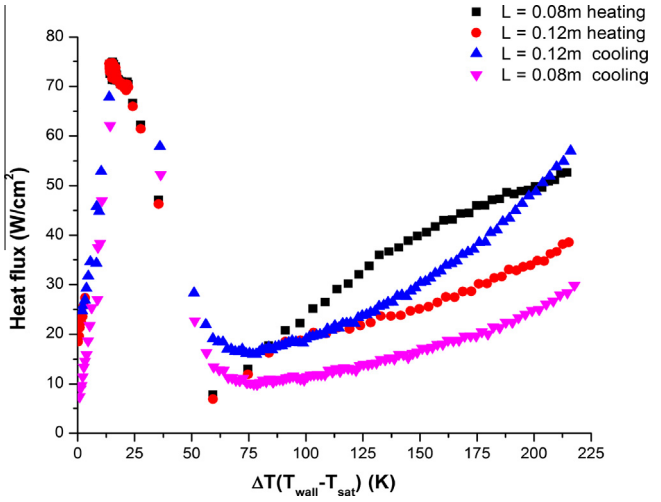

Fig. 6. Heating and cooling curves for varying L values.

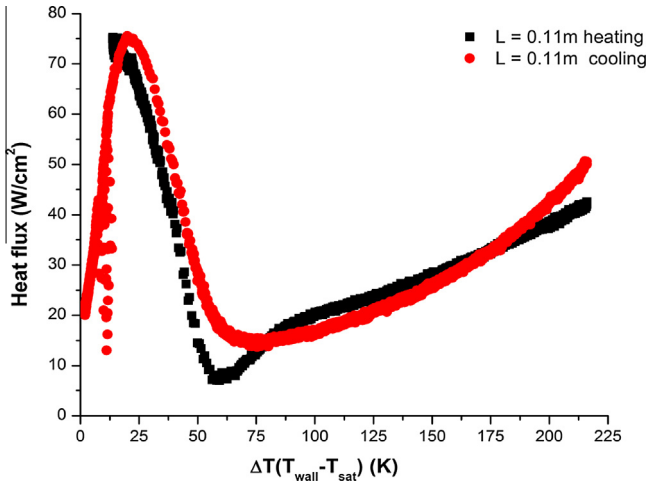

Fig. 7. Heating and cooling curve for L = 0.11 m.

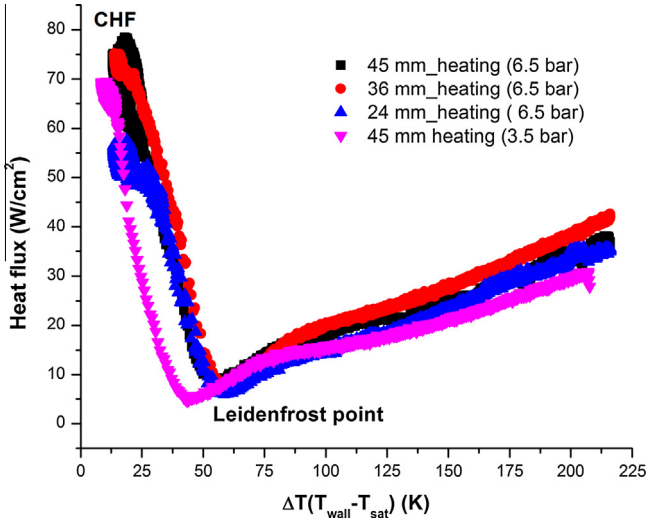

Fig. 8. Liquid nitrogen boiling curves.

L = 0.12 m, the heat flux values are lower for heating compared to cooling. However at L = 0.11 m, the values of heat flux for heating and cooling are close to each other, and the differences are within the uncertainty range. A useful metric that can be adopted is to find the corresponding heat flux for a given superheat and see at how the heat flux estimated by cooling curve and heating curve match. This process is carried out for many superheat values which are spaced at intervals of 10 K from 25 K to 200 K. The length of copper block which results in maximum no of points having such close prediction (difference is less than uncertainty error) between heating and cooling transient is considered as the actual representative length. Another useful way to confirm this is to compare the cooling curve in nucleate boiling regime with the heat fluxes obtained from steady state temperature measurements in this region. Hence for future calculations for heat transfer coefficients, L = 0.11 m was used.

Fig. 8 shows the boiling curve beyond CHF for various cases – different nozzle heights and spray pressures - (24/36/45 mm heights at 0.65 MPa and 45 mm height at 0.35 MPa). The maximum heat flux values range between 55 W/cm^2 (at ΔT of 15 K for H = 24 mm) to 77 W/cm^2 (at ΔT of 19 K for h = 45 mm). The Leidenfrost point (point of minimum heat flux and the surface being completely covered by a vapor blanket) was in the region of

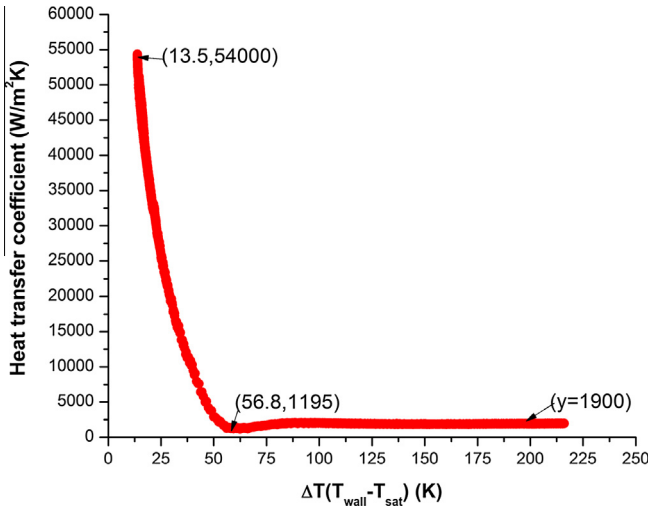

Fig. 9. Heat transfer coefficient variation with wall temperature.

ΔT = 56 K (i.e. at −140 °C). A lower pressure spray (0.35 MPa, H = 45 mm) reached critical heat flux with a heat flux of 69 W/cm^2 and Leidenfrost point was also reached early at ΔT = 44 K.

Fig. 9 shows the variation of heat transfer coefficient for wall temperatures above the CHF, for an inlet pressure of 0.65 MPa at 36 mm nozzle height with a flow rate of 26 kg/h. The heat transfer coefficient is typically about 40,000–55,000 W/m^2 K near the CHF region and decreases rapidly in the transition boiling region. It reaches the minimum values of about 1200 W/m^2 K at the Leidenfrost point and remains constant at about 1900 W/m^2 K in the film boiling regime.

8. Conclusion

Thus an easy and novel way to construct the full boiling curve for refrigerants was demonstrated. The method is quick and easy to implement and specifically suitable for forced convection boiling such as spray cooling. By using this method, the spray boiling curve for liquid nitrogen is reported for the first time in literature. Such full boiling curve gives an estimate of minimum heat flux, Leiden frost point and the film boiling heat transfer coefficients.

References

[1] S. Nukiyama, The maximum and minimum values of the heat Q transmitted from metal to boiling water under atmospheric pressure, Int. J. Heat Mass Transf. 9 (12) (1966) 1419–1433.
[2] T.B. Drew, A.C. Mueller, Boiling, Trans. Am. Inst. Chem. Eng. 33 (1937) 0449–0473.
[3] E.K. Ungar, R. Eichhorn, Transition boiling curves in saturated pool boiling from horizontal cylinders, J. Heat Transf. 118 (3) (1996) 654–661.
[4] H. Tatsumoto, Y. Shirai, K. Hata, T. Kato, M. Shiotsu, Forced convection heat transfer of subcooled liquid nitrogen in horizontal tube, AIP Conf. Proc. 985 (2008) 665.
[5] M. Shiotsu, H. Kobayashi, T. Takegami, Y. Shirai, H. Tatsumoto, K. Hata, et al., Transient heat transfer from a horizontal flat plate in a pool of liquid hydrogen, AIP Conf. Proc. 1434 (2012) 1059.
[6] I.I. Petukhov, V.N. Syryi, S.D. Frolov, M.A. Turnov, Investigation of boiling of cryogenic liquids, Heat Transf. Res. 27 (1) (1996) 261–264.
[7] M. Ohya, K. Hata, M. Shiotsu, Transient heat transfer from a flat plate in a pool of FC-72, in: Proceedings of IPACK'01 – The Pasific Rim/ASME International Electronic Packaging, 2001, pp. 753–761.
[8] D.N.T. Nguyen, R.H. Chen, L.C. Chow, C. Gu, Effects of heater orientation and confinement on liquid nitrogen pool boiling, J. Thermophys. Heat Transf. 14 (1) (2000) 109–111.
[9] Y. Guo, Q. Bi, T. Chen, Nucleate pool boiling heat transfer of liquid nitrogen in combinative surface tube bundle, Huagong Xuebao/J. Chem. Ind. Eng. (China) 55 (9) (2004) 1417–1421.

[10] M.C. Duluc, M.X. Francois, J.P. Brunet, Liquid nitrogen boiling around a temperature controlled heated wire, Int. J. Heat Mass Transf. 39 (8) (1996) 1758–1762.
[11] M. Ciofalo, A. Caronia, M. Di Liberto, S. Puleo, The Nukiyama curve in water spray cooling: its derivation from temperature-time histories and its dependence on the quantities that characterize drop impact, Int. J. Heat Mass Transf. 50 (25–26) (2007) 4948–4966.
[12] D. Quéré, Leidenfrost dynamics, Annu. Rev. Fluid Mech. 45 (2013) 197–215.
[13] S. Somasundaram, A.A.O. Tay, A study of intermittent spray cooling process through application of a sequential function specification method, Inverse Probl. Sci. Eng. 20 (4) (2012) 553–569.
[14] J.V. Beck, B. Blackwell, C.R. St-Clair Jr., Inverse Heat Conduction: Ill-Posed Problems, Wiley Intersciences, New York, 1985.